Fragility and climate impact assessment of contemporary housing roof sheeting failure due to extreme wind

Mark G. Stewart[a,*], John D. Ginger[b], David J. Henderson[b], Paraic C. Ryan[c]

[a] Centre for Infrastructure Performance and Reliability, The University of Newcastle, New South Wales 2308, Australia
[b] Cyclone Testing Station, James Cook University, Townsville, Australia
[c] Discipline of Civil, Structural and Environmental Engineering, School of Engineering, University College Cork, Ireland

ABSTRACT

The paper describes a risk analysis of the economic impact of damage to metal roofing of a typical contemporary (new) Australian house subject to extreme wind loading. The failure modes considered are roof cladding and batten-to-truss connection failures, with the effect of defective construction also considered. Monte-Carlo simulation and structural reliability methods are used to stochastically model spatially varying pressure coefficients, roof component failure, and load re-distribution across the roof. This spatial reliability analysis enables fragility curves to be developed that relate likelihood and extent of roof cover loss to gust wind speed. The annual economic risk is up to 0.3% of house replacement value. A typical house with construction defects increases economic risk more than sixfold when compared to the defect-free house. There is a 10% chance that a changing climate will increase expected losses for houses in Brisbane and Melbourne by 6–18% over the next 50 years.

1. Introduction

Severe storms (excluding tropical cyclones) cause insured losses of nearly $400 million annually in the Australian states of Queensland, New South Wales and Victoria [5]. These losses account for nearly 25% of all losses from natural disasters in Australia. Most damage occurs to housing (e.g. [25,32]). Climate change-induced increases in wind speed may occur in some regions of Australia [58]. An improved understanding of the vulnerability of housing to wind damage is key to assessing the current and future impacts of climate change, as well as deciding if it is cost-effective to implement design or construction changes to reduce climate change impacts (e.g., [48,49,50]).

Wind fragility expresses building damage as a function of wind speed. Engineering fragility, vulnerability, and risk assessment models have been developed for different types of structures which use reliability-based methods (e.g., [55,20,29,33,53,34,38,12,59,6,43,9]). Many of these models are developed for timber roof sheathing which is representative of housing in hurricane prone regions of North America, and some of these studies include the effect of climate change. In Australia, many houses have metal roof cladding. Much research has focused on roofing vulnerability as this is an important indicator of loss, for example, HAZUS [18] estimates total loss of building interiors and contents with 25% loss of roof covering. Few engineering fragility

models are publicly available for Australian buildings. Henderson and Ginger [20] developed a reliability-based engineering fragility model for the older, more vulnerable Australian high-set houses against cyclonic wind loading. This study examined metal roof cladding pulling over fixing, cladding fastener failure, batten joint failing at rafter and rafter joint failing at ridge, and assumed a relatively simple series system based on the weakest-link hypothesis. However, load redistribution based on progressive failure load paths, spatial distribution of wind load, internal pressure variation caused by the roof sheeting failure, sheet failure criterion, and construction defects were not considered. Konthesingha et al. [28] has implemented some of these features into the fragility analysis of low rise metal-clad industrial buildings, however, the analysis ignored construction defects.

Housing losses due to extreme wind events often accrue to damage to the roof envelope [21,7]. Consequently, the paper herein focuses on the roof structure of a typical Australian house. The dominant failure modes considered in this study are (i) roof cladding failure, and (ii) batten-to-truss connection failure. The effect of defective construction at connections on wind fragility is also considered. Monte-Carlo simulation and structural reliability methods are used to stochastically model spatially varying pressure coefficients, roof component failure for 1600 roof fasteners and 500 battens, load re-distribution across the roof as connections progressively fail, loss of roof sheeting as a critical

---

number of connections fail, and changes in internal pressure coefficient with increasing roof sheeting loss. Fragility curves can then be developed that relate likelihood and extent of roof cover damage with wind speed. Housing representative of contemporary (new) houses in the Australian cities of Brisbane and Melbourne are considered, and houses in these regions are classified by the Australian wind loading standard AS/NZS1170.2 [3] as non-cyclonic. As noted above, most wind fragility analyses in the literature focus on extreme winds caused by hurricanes or cyclones. Houses in these regions in the United States and Australia tend to be constructed to higher standards. However, in Australia more than 95% of the population live in non-cyclonic regions, and wind damage to these houses can also be significant (e.g., [32]).

Finally, a risk assessment is conducted to assess the risks and economic impact of roof cladding wind damage. Roof cover loss includes structural, interior, contents, and loss of use losses. The economic risks are calculated as the product of hazard likelihood, fragility, and loss, over the 50-year design life of residential houses designed to be nominally sealed. The effect of climate change on wind speed and damage risks is also considered.

2. Risk, fragility and vulnerability

The risk from extreme wind events is:

$$E(L) = \sum Pr(H)Pr(DS\,|H)Pr(L|DS)L \qquad (1)$$

where $Pr(H)$ is the annual probability of a hazard (wind speed), $Pr(DS|H)$ is the damage state probability conditional on the hazard (also known as fragility), $Pr(L|DS)$ is the conditional probability of a loss given occurrence of the damage, and L is the loss or consequence if full damage occurs. The summation sign in Eq. (1) refers to the number of possible hazards, damage states and losses. If the loss refers to a monetary loss, then $E(L)$ represents an economic risk.

The probability of component failure (p_f) is:

$$p_f = Pr[R-(W-D_L) \leqslant 0] \qquad (2)$$

where R-$(W$-$D_L)$ is the "limit state function" equal to resistance minus load, R represents resistance of the element considered, W is the uplift wind load, and D_L is the roof dead load. The dead load is considered to be deterministic. However, resistance and wind load are modelled probabilistically due to their high levels of variability and uncertainty. The fragility is defined as damage likelihood at a specific wind speed v, where damage state DS is measured by proportion of roof sheeting loss (R_{damage}) which is based on the number of roof sheets which have failed at a given wind speed, giving

$$Pr(DS|H) = Pr[DS=R_{damage}\,|H= v] \qquad (3)$$

A roof sheet is defined to have failed (i.e. loss of entire roof sheet) herein, when a predetermined number of fasteners fail in each roof sheet. The probabilistic model examines roof failure down to the cladding and batten fastener element level, facilitating the detailed incorporation of load re-distribution and spatial variability across the roof as fasteners progressively fail. Event-based Monte-Carlo simulation methods are used to model damage progression and hence the estimation of fragility $Pr(DS|H)$ for gust wind speeds of up to 80 m/s. The simulation analysis allows for the spatial distribution of wind loads across the roof. This event-based methodology then allows the consequences of a given failure event to be incorporated into the model as wind speed increases. For instance, when a fastener fails at a given wind speed, its load is re-distributed to adjacent fasteners for subsequent wind speeds. The event-based approach also allows for changes in internal wind pressure with roof sheet failure to be incorporated into the model. The event-based simulation flowchart of the fragility model is described in Fig. 1.

3. Wind hazard and climate change

Non-cyclonic gust speeds (winds not associated with tropical cyclones) dominate in South-East Queensland, and further south in Melbourne. The latest Australian Commonwealth Scientific and Industrial Research Organisation (CSIRO) projections for changes in annual peak gust wind speeds for Brisbane and South-East Queensland (this region accounts for nearly 20% of the population of Australia) are provided by Dowdy et al. [11] and summarised in Table 1 for low, medium and high CO_2 emission scenarios RCP2.6, RCP4.5 and RCP8.5, respectively, to 2090. Note that climate projects are relative to 1995 levels (1986–2005 average), and the Australian Government uses CSIRO projections for their climate impact modelling. It is clear from Table 1 that "projections of extreme winds indicate that reductions are more likely than increases based on the model ensemble median" [11]. On the other hand, extreme wind projections for Melbourne are less clear, and "extreme winds could increase or decrease" [17]. For this reason, projections for annual peak gust wind speeds in Melbourne are provided by CSIRO only for RCP8.5 (see Table 1). It is important to note that the wind projections for much of the coastal region of Victoria and New South Wales are very similar to those for Melbourne (this region accounts for over 40% of the population of Australia). It is also noted that "The projections of extreme winds are less certain than for other variables since there is a limited number of GCMs (general circulation models) that provide wind data, and maximum wind speed needs to be estimated using indirect means" [17]. The cumulative distribution function for annual maximum non-cyclonic peak gust speed [57,49] is modified as:

$$F_V(v, t) = e^{-e^{-A}} \text{where } A= \frac{\left(\frac{v}{1 + \frac{\gamma_{mean}(t)}{100}}\right)-v_g}{\sigma_g} \qquad (4)$$

where v_g and σ_g are the location and scale parameters, respectively ($v_g = 26.0326$, $\sigma_g = 4.0488$ for Brisbane and $v_g = 27.7777$, $\sigma_g = 1.664$ for Melbourne), $\gamma_{mean}(t)$ is the time-dependent percentage change in gust wind speed, and gust wind speed v is the maximum 0.2 s gust velocity at 10 m height in Terrain Category 2 (open terrain defined in [3]). Fig. 2 shows the relationship between gust wind speed and return period calculated from Eq. (4) when $\gamma_{mean}(t) = 0$. Information is scarce to non-existent on time-dependent changes in wind speed for Australia. A time-dependent linear change in wind speed is assumed as it has been shown that the effect of a non-linear time-dependent change in wind speed has a minor influence on damage risks even when investigated for a wind speed change scenario of + 20% (e.g., [47]). In the present case, the projected changes in wind speed over the next 50 years are less than 4%, hence, results will be insensitive to assumptions about the nature of the time-dependent increase in wind speed.

4. Fragility analysis

4.1. Representative house

Field surveys of contemporary houses being built in the suburbs of Brisbane and Melbourne were completed in 2014 by the Cyclone Testing Station (CTS) at James Cook University (JCU) as part of a CSIRO Climate Adaptation Engineering for Extreme Events (CAEx) project [39]. It was found that houses in Melbourne are of similar size, shape and construction type to houses in Brisbane. The data from this detailed survey was used to define a representative house. Median values of variables such as footprint dimensions, roof pitch, and wall heights were selected to determine the dimensions of the representative houses. These houses are, in general, designed to be nominally sealed.

Fig. 3 shows the representative 1-storey Brisbane/Melbourne house. It is timber framed brick-veneer construction with a 21.5° timber roof truss (at 600 mm spacings) on a complex hip-end roof. Trusses are
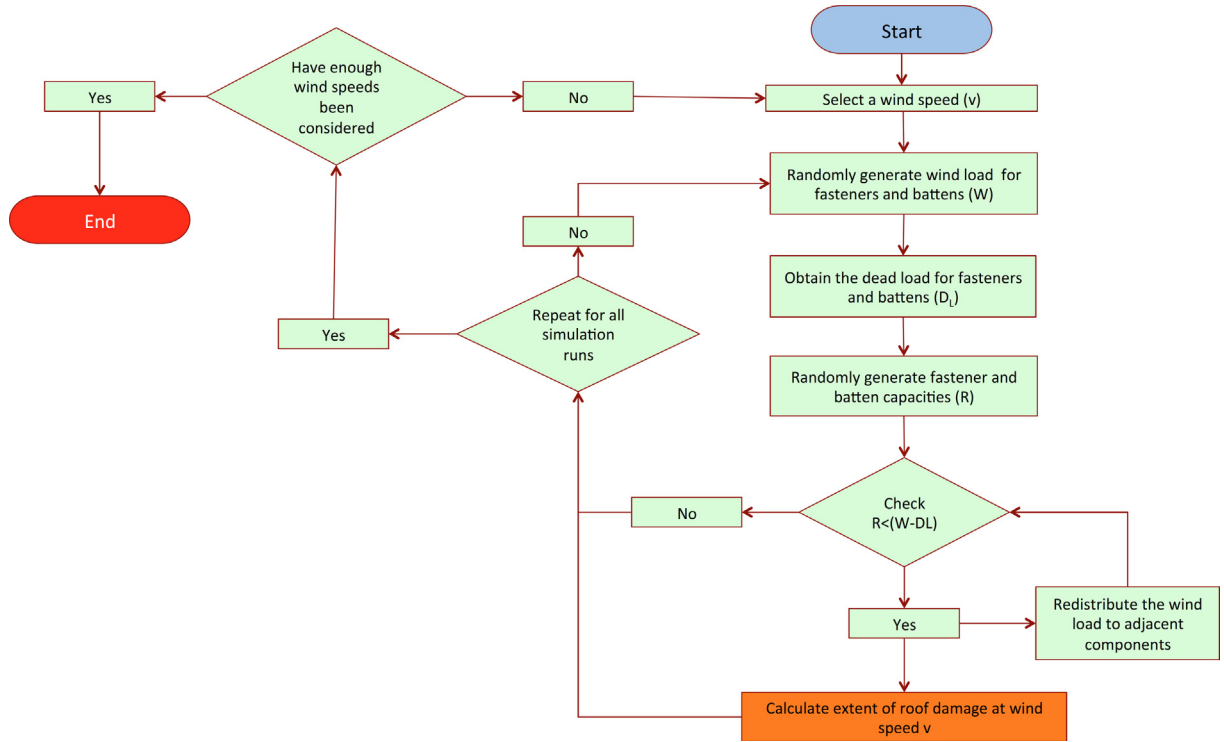
Fig. 1. Flowchart of the fragility model.

Table 1
Change in wind speeds γ_{mean} (2090) for three emission scenarios.

Location	RCP2.6			RCP4.5			RCP8.5		
	10th	Median	90th	10th	Median	90th	10th	Median	90th
Brisbane	−2.5%	0.0%	+2.5%	−8.0%	−1.5%	+1.0%	−5.0%	−2.0%	+2.0%
Melbourne	NA	NA	NA	NA	NA	NA	−4.0%	−1.0%	+5.0%
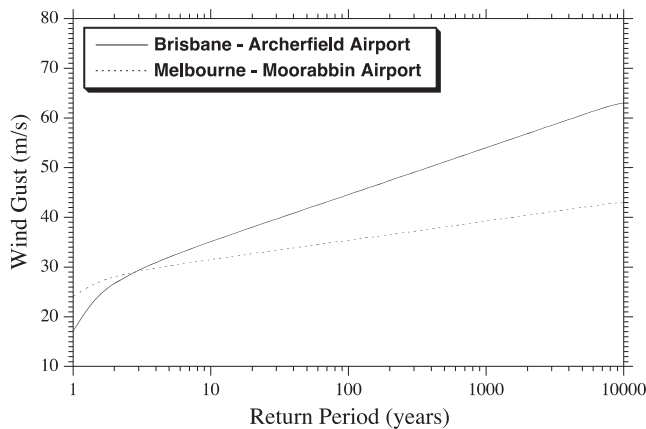
Fig. 2. Influence of return period on gust wind speed.

Fig. 3. Representative 1-storey house.

arranged with general trusses in the middle part of the roof and jack trusses connected to girder trusses at the hip-ends. Fig. 4 shows the typical structural system of the representative house.

4.2. Wind loading

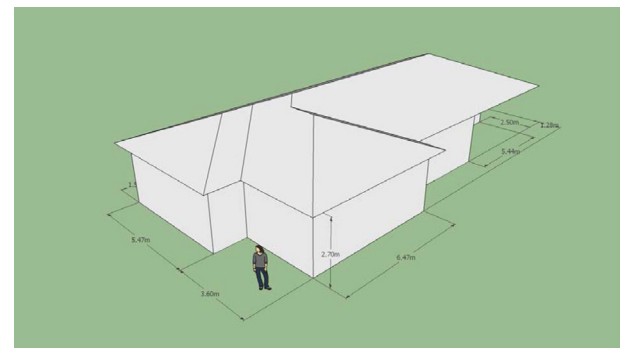The wind load (W) is modelled probabilistically as [24]:

$$W = Bv^2 \tag{5}$$

where v is the maximum 0.2 s gust velocity at 10 m height in Terrain Category 2 (i.e. open terrain). The parameter B is:

$$B = \lambda \cdot M \cdot A \cdot \left(C \cdot T \cdot E^2 \cdot D^2 \cdot G \cdot \frac{\rho}{2} \right) \tag{6}$$

where *C* is the quasi-steady pressure coefficient, *E* accounts for the exposure and height of the building considered, *T* is a shielding factor, *D* is a factor for wind directionality effects, *G* is a factor to incorporate the spatially and temporally varying pressures across the building envelope, ρ is the density of air, *A* is the tributary area, λ accounts for wind load modelling inaccuracies and uncertainties in analysis methods, and M accounts for wind tunnel modelling inaccuracies such

Fig. 4. Truss roof and timber frame of single storey house in Brisbane.

Table 2
Statistical parameters for wind loading.

Parameter	Nominal value	Mean-to-nominal	COV
λ/λ_N	1.0	1.0	0.10
M/M_N	1.0	1.0	0.10
A/A_N	Tributary area	1.0	0.10
E/E_N	0.87	0.95	0.10
T/T_N	1.0	1.0	0.10
D/D_N	1.0	1.0	0.00
G/G_N	1.0	1.0	0.05
ρ/ρ_N	1.2 kg/m^3	[43]	0.02

as incorrect Reynolds number, building details, and site modelling. These parameters, with the exception of C, are assumed to have a lognormal probability distribution with statistical parameters given in Table 2, for more details see Henderson and Ginger [20] and Holmes [24]. Nominal values are obtained from the Australian wind loading standard AS/NZS1170.2 [3]. Random variables λ, M, E, T, D, G and ρ are statistically independent for each simulated house, but then fully correlated for each fastener in the simulated house. The nominal tributary area (A_N) per fastener is taken as batten spacing × width of the sheeting between fasteners [22], and A is statistically independent for each fastener. If one or two of the random variables given in Table 2 are assumed as deterministic, fragilities and economic risks reduce by less than 2%.

4.2.1. External pressure coefficients

A wind tunnel model of the 1-storey representative Brisbane/ Melbourne house was constructed at a length scale of 1/50, as shown in Fig. 5 (see [16,39]). Three hundred and twenty pressure taps were installed on the external roof surface to measure the spatial and temporal variation in external pressure. An Alfresco area (covered open area), typical of contemporary Australian housing, was modelled at the rear of the house, see Fig. 6. Pressure taps are arranged on the model in a 12 mm × 18 mm grid-pattern (representative of the 600 mm × 900 mm truss-batten spacings in full-scale) as shown in Fig. 6 to enable cladding

Fig. 5. Wind tunnel model of 1-storey Brisbane/Melbourne house.

loads, batten-truss loads and the resulting wind load effects on the trusses to be determined. The tests were conducted in the 2.0 m high × 2.5 m wide × 22.5 m long Boundary Layer Wind Tunnel at JCU.

The design suction pressures on the roof were obtained by extracting the largest peak suction pressure coefficient, for each tap on the roof surface for each wind direction (θ of 0° to 350° at intervals of 10°), see Fig. 7. As expected, Fig. 7 shows that measured peak suction pressures are spatially variable, are highest at roof edges, hips and ridgelines, and are highly influenced by wind direction. For more details of the testing see Ginger et al. [16] and Parackal et al. [39].

Statistical parameters for peak suction pressure values (C_{peak}) were obtained from the peaks observed for three sequential sets of 10 min wind tunnel observation data for each tap location for each direction. The wind tunnel pressure coefficient data are assumed to have an Extreme Value Type 1 (Gumbel) probability distribution (e.g. [41]). Due to the relatively small sample size, the analysis includes a combined coefficient of variation (COV) of 0.15 to allow for wind tunnel modelling inaccuracies, spatially and temporally varying pressures across the building envelope, and wind load modelling uncertainties, see Table 2.

Clearly, peak pressures across a roof surface will not occur simultaneously at the same point-in-time. However, each tap is highly likely to experience a peak pressure over the duration of that wind event. Hence, fasteners and battens that experience loading from peak pressure recorded at a single tap will all experience peak uplift – although not at the same point-in-time. Hence, some fasteners may experience peak uplift early on, some may even fail and redistribute loads to adjacent fasteners, while seconds later other fasteners may experience their peak uplift, may fail, redistribute loads, etc. Wind tunnel testing has shown that there is very high correlation of C_{peak} values between taps in edge zones – i.e., a correlation coefficient of 0.9 [13]. These are the regions where failure is initiated, and so assuming simultaneous peaks over small areas (fasteners and battens) is a reasonable, albeit slightly conservative, assumption [28]. Hence, the present analysis assumes a correlation coefficient of 0.9 for all pressure tap data. It is noted that calculated fragilities are not sensitive to assumptions about the pressure tap correlation coefficient [51].

4.2.2. Internal pressure coefficient

Progressive failure of the roof envelope (i.e. loss of roof sheeting) is likely to change internal pressures [56,28]. Fig. 8 shows the mean change in internal pressure (C_{pi}) due to loss of roof sheeting with, and without, a large dominant opening (i.e. failed doors or windows in the house due to wind-borne debris) in the windward wall. When there is no loss of roof sheeting, Fig. 8 is based on internal pressure coefficients obtained from AS/NZS1170.2 [3], and is assumed that the dominant opening is located in the centre of a wall (e.g. [51]). As roof sheets start to fail, Fig. 8 is based on wind tunnel data (see Section 4.2.1) and expert judgement. Analysis of the wind tunnel data shows that measured pressures are very similar to design code values with an accuracy of ± 0.1. For example, Fig. 8 is applicable for winds from any direction – e.g., a wall is defined as 'windward' if the wind direction is ± 45° to the wall's orthogonal direction. Variability of C_{pi} is low for an intact roof [14], and so is modelled as a normal distribution with an assumed standard deviation of $\sigma_{Cpi} = 0.1$. Loss of roof sheeting will result in higher variability of internal pressures, leading to an assumed higher $\sigma_{Cpi} = 0.2$. A sensitivity analysis shows that results are not sensitive to σ_{Cpi} if $\sigma_{Cpi} \leq 0.2$. Improving Fig. 8 is an area for further research.

4.3. Resistance

The representative Brisbane/Melbourne house has 0.42 mm metal corrugated sheeting secured by screw fasteners at every 2nd corrugation (150 mm spacing) for edge battens, and every 3rd or 4th corrugation for other regions of the roof (i.e., 3–4–3 fixing pattern per sheet). Fig. 9 shows, for illustrative purposes, the batten, sheet, and fastener
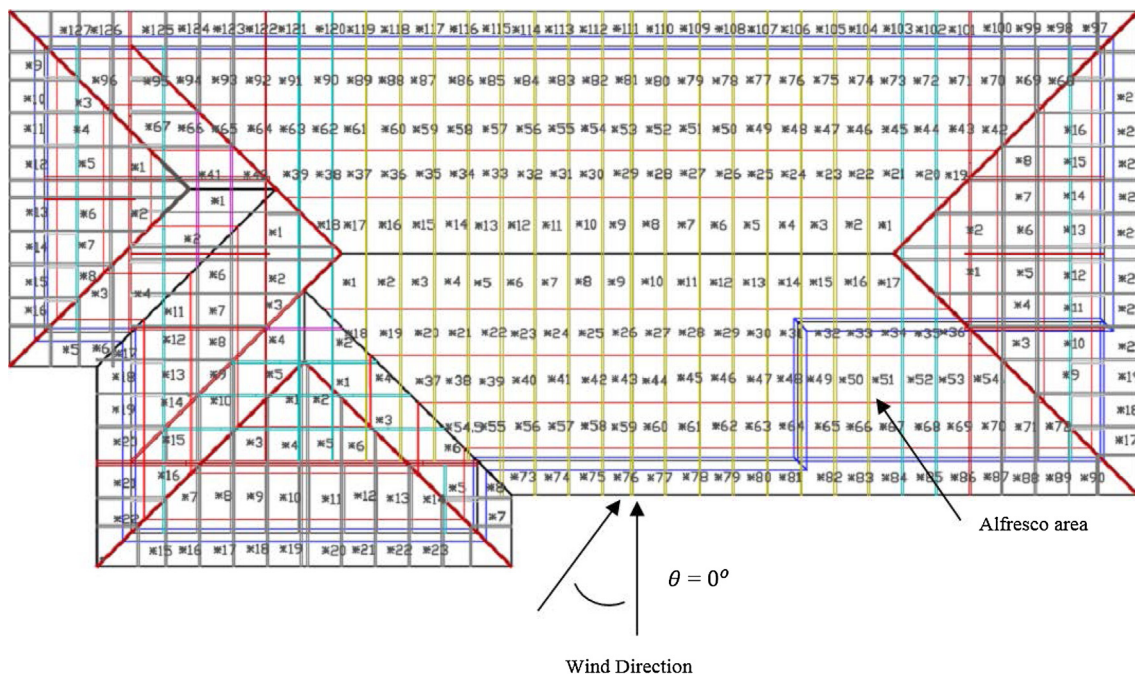
Fig. 6. Layout of pressure taps superimposed on roof framing plan.

layout showing screw fasteners at every 2nd corrugation. Roof battens are 0.55 mm metal top-hat 40 battens at 900 mm centres secured to every truss with 6 mm diameter screw fasteners [35]. Soft wood pre-fabricated trusses are spaced at 600 mm. Roof sheeting and batten connections are identical for Melbourne and Brisbane houses [39].

4.3.1. Component capacities

Probabilistic data for roof fasteners consider two failure modes: (i) pull-over and (ii) pull-out failures. These are inferred from Mahendran [36], Mahendran and Tang [37] and test data. Batten-to-truss connection capacities also consider two failure modes obtained from (i) pull-over and (ii) pull-out failure test data [8]. Table 3 summarises the statistical parameters for component capacities. Component capacities are assumed statistically independent and taken as the lower of randomly generated pull-out and pull-over capacities. Component capacities are assumed lognormally distributed [19].

4.3.2. Fastener and batten failure progression

When a roof fastener fails, Henderson and Ginger [22] found that the load is distributed to adjacent fasteners as shown in Fig. 9 which shows how failure of Fastener A results in its load being distributed to adjacent fasteners. A batten failure is modelled as if all roof fasteners connected to the batten have failed. For more details of load redistribution see Konthesingha et al. [28]. The probabilistic representation of over 1600 roof fasteners and 500 battens requires event-based modelling of fastener and batten failure progression for each increment of wind speed. The load is redistributed to other connections as more connections fail, which can then overload nearby connections that may then lead to 'unzipping' of connections and rapid damage progression.

4.3.3. Sheet failure criterion

The number of failed fasteners to cause loss of an entire roof sheet is defined herein as the sheet failure criterion (or SFC). The SFC is a difficult parameter to determine as it can differ depending on wind direction, roof sheet dimensions, location of the failed fasteners in the sheet, wind pressure distribution along the sheet, etc. Konthesingha et al. [28] based fragility modelling of metal clad industrial buildings on a 20% SFC. A reasonable lower bound for SFC assumes two fasteners cause roof sheet failure in line with Henderson et al. [23] which

represents SFC = 10%. The upper bound assumes that 80% of fasteners must fail to cause roof sheet failure [18]. The evidence suggests that failure of a few fasteners will result in sheet failure rather than failure of many fasteners [28]. Hence, a triangular probability distribution for SFC is adopted herein bounded by 10% and 80% (average is 33.3%), see Fig. 10. A sensitivity analysis shows that results are not sensitive to SFC (for more details see [28]), but SFC is clearly an area for further research.

4.3.4. Human error and construction defects

It is generally accepted that design and construction errors are the dominant cause of structural failures, and so humans are the 'weakest link' in the design and construction process [45]. Moreover, defects are typically observed in housing construction (e.g., [15,31,26]). In Australia, this may include roofing screws misaligned (not centred on crest of corrugation) or missing the batten completely, batten fasteners missing or not centred properly, and inadequate tie-down connections between roof truss and wall (e.g., [32]). Clearly, when modelling the failure and vulnerability of houses due to extreme wind it is desirable to include the effects of human error in construction [30,26,54]. The Human Reliability Analysis (HRA) approach is suitable for probabilistic modelling construction errors in a risk analysis [46].

The statistical parameters for fastener capacities shown in Table 3 describe results of testing of connections constructed in the laboratory with good quality workmanship. In this case, a 'defect' may be defined as one that causes a loss of capacity in exceedance of acceptable variability or tolerance. If we assume a lower bound of acceptable variability is the 1st to 5th percentile of the lognormal distribution of fastener capacities described in Table 3, then this relates to a minimum capacity reduction of 28–50% for roofing fasteners, and 22–37% for batten connections. Hence, minimum capacity reductions due to defects for roofing fasteners and batten connections are taken as 40% and 30%, respectively. The most likely capacity reduction for a roofing fastener is 100% as this relates to a screw fastener not attached to the batten or the fastener simply not installed. Two screws comprise a batten-to-truss connection, so a likely scenario may be the incorrect installation of both screws (installed at angle, or not centred), or one missing screw leading to a capacity reduction of 50%. Capacity reductions are modelled as triangular probability distributions as shown in Table 4. In this case, the
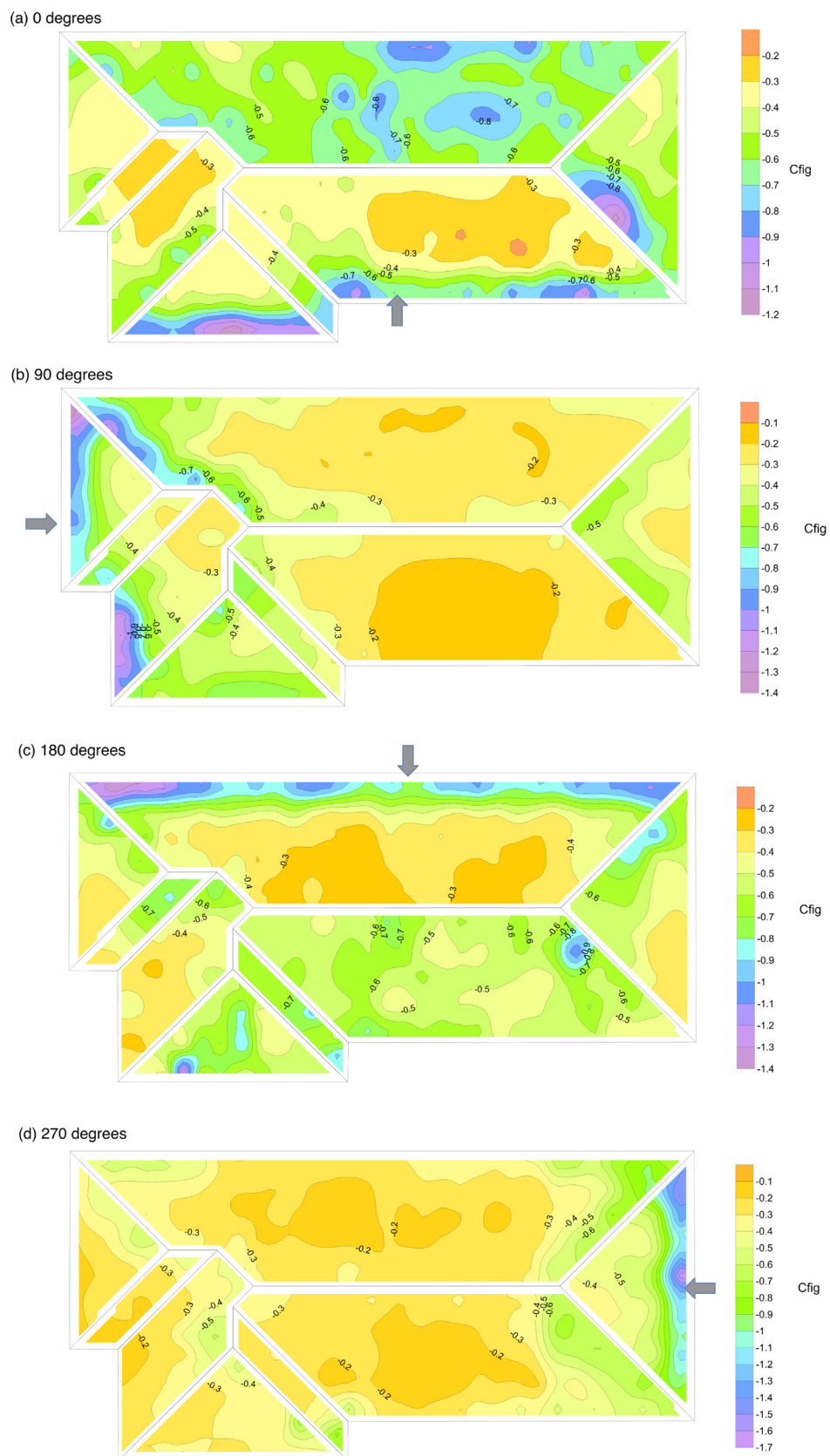
(a) 0 degrees

(b) 90 degrees

(c) 180 degrees

(d) 270 degrees

Fig. 7. Peak external suction pressure coefficients on 1-storey house – wind tunnel study for four wind directions: (a) 0˚, (b) 90˚, (c) 180˚, and (d) 270˚.
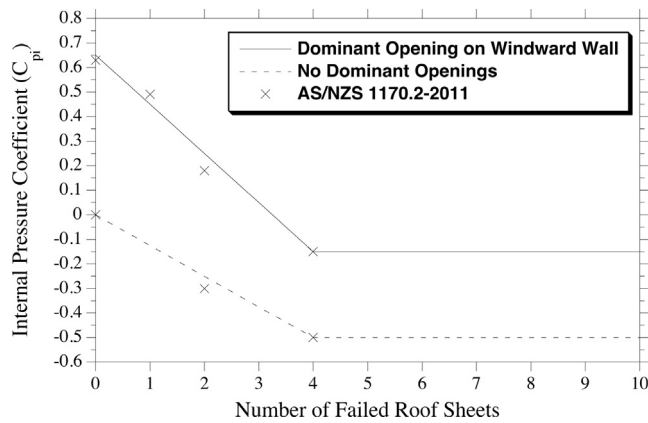
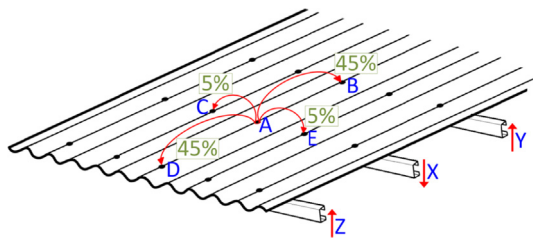**Fig. 8.** Effect of failed roof sheeting on internal pressure coefficient.

Fig. 9. Load redistribution of failed fasteners or battens.

Table 3
Statistical parameters for fastener and batten resistance.

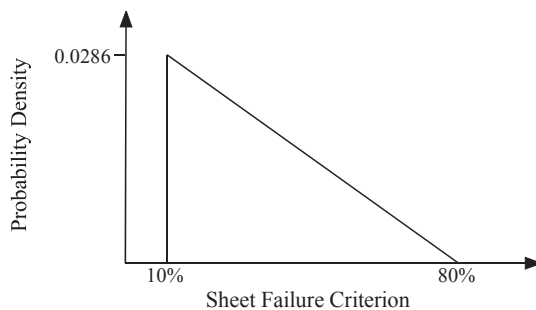| Component and failure mode	Mean	COV
Roof fastener:		
(i) roof sheeting pulling over fastener	1.2 kN	0.3
(ii) roof fastener pulling out of roof batten	1.2 kN	0.2
Batten-to-truss connection:		
(i) batten pulling over fastener	4.5 kN	0.15
(ii) batten fastener pulling out of roof truss	5.5 kN	0.2

Fig. 10. Triangular probability distribution of sheet failure criterion.

mean capacity reduction is 80% and 60% for roof fasteners and batten connections, respectively.

Data on defect rates is more difficult to infer. Hong and He [26] conducted a statistical analysis of missing nails (i.e., nails at specific locations are required but missing) and improperly fastened nails (i.e., nails that have penetrated to the roof panels but missed the roof trusses) in a timber sheath roof constructed in a laboratory in Canada. They found an error rate of 1.5%, with 80% of errors relating to improperly installed nails missing the roof truss. Hong and He [26] state that since their statistics are based on a laboratory setting the 1.5% error rate is perhaps closer to a lower bound, and so we consider lower and upper bounds of 1% and 3% respectively. The task of installing metal roof

cladding is different of course, for example, there may be higher accuracy of inspecting the location of roof fasteners as a fastener not connected to a batten will look out of line with other fasteners, but data from Hong and He [26] provide a useful benchmark for our analysis, and as noted by Leitch et al. [32] roofing screws installed in Australia, like nails, may also miss the batten. Hence, the present analysis assumes a fastener defect rate of 1–3% assumed uniformly distributed. Batten-to-truss connections may be more difficult to inspect visually, and involve the installation of two screws – defect rates are likely to be higher. Hence, we assume double the defect rate than that of fasteners (2–6%) and also assumed to be uniformly distributed. Table 4 shows the defect rates and capacity reduction for components considered in the present paper.

There is much research to show that defects are correlated or dependent – i.e. one error or defect is more likely to lead to other errors or defects. Hence, some houses are likely to have many defects, others very few if any. The clustering of defects may be due to differing work practices between builders, differing levels of inspection, or the effect of individuals with poor construction techniques. The probability of a defect given a defect on the previous task is obtained from the following standard HRA technique [27]:

$$\text{Pr(defect | defect on previous task)} = \left(\frac{1 + A \cdot \text{defect rate}}{A+1} \right) \quad (7)$$

where A = 19, 6 and 1 for low, moderate and high dependence. For example, a moderate dependence and a defect rate of 1.5% leads to Pr (defect | defect on the previous task) = 15.6%. Moderate dependence is assumed in the present analysis, and roof fasteners and batten connection defect rates are fully correlated. The quantification of defects given in Table 4 is intended to start a discussion about defects and their probabilistic quantification. There is a clear need for the collection of field data on construction defects, although collecting unbiased human error or construction defect data can be problematic (e.g., [44,45]), but is necessary to better quantify defect rates and their magnitude.

5. Results – fragility curves
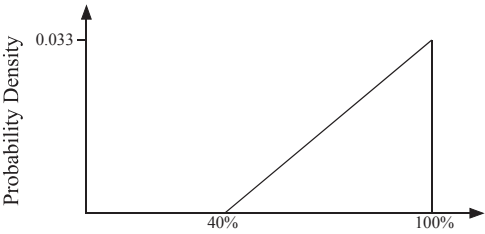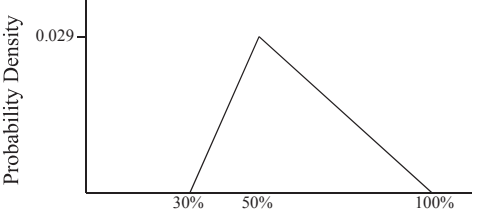
5.1. Design considerations

The terrain multiplier specified in the Australian Standard "Wind Loads for Houses" [4] is $E_N = 0.87$ for suburban housing, see Table 2. For a typical suburban development, [4] specifies that there is no shielding of the roof from nearby houses and so $T_N = 1.0$.

A dominant opening on the windward wall can cause large roof uplift and roofing damage (e.g., [32]). For many houses, this manifests as damage to windows and doors which can cause large uplift to the ceiling that can lead to failure of the truss-to-wall connections. This is also likely to lead to failure of the access hole to the ceiling and then large internal uplift on the roof. The fragility due to presence and absence of openings in the building envelope (e.g., door failure, window breakage, openings not closed) is also analysed.

Unless noted otherwise, wind direction is uniformly distributed in 10° increments between 0° and 360° to allow for variability of building orientation – this allows for fragilities to be assessed for a house for a specific wind speed. In other words, 5000 Monte-Carlo simulation runs are conducted for each wind direction, and then the multi-directional fragility is the average fragility of all these Monte-Carlo simulation runs (i.e., 36 × 5000 = 180,000 runs). The directionality of the wind climate will be added to the fragility analysis described herein to represent average loss (see Section 7). Doors and/or windows are located on all exterior walls of most detached houses. Hence, if a dominant opening is to occur, it is assumed herein to occur on the windward wall as this is the wall orientation most vulnerable to flying debris and large wall pressures (e.g., [32,40]).

Note that the loss of many roof sheets will significantly alter

Table 4
Defect Rates and Capacity Reduction.

Component	Defect Rate per component	Probability distribution of capacity reduction
Roof fastener	1–3%	
Batten-to-truss connection	2–6%	

aerodynamic behaviour of the roof, and change internal and external pressures from that assumed in Figs. 7 and 8. Hence, there is lower confidence in fragilities in excess of 10–20%. This is of little practical significance for loss and cost-benefit modelling, however, as roof sheeting is entirely replaced when roof cover damage exceeds 5%, and building interior and contents losses reach 100% when roof cover damage exceeds 25% [18].
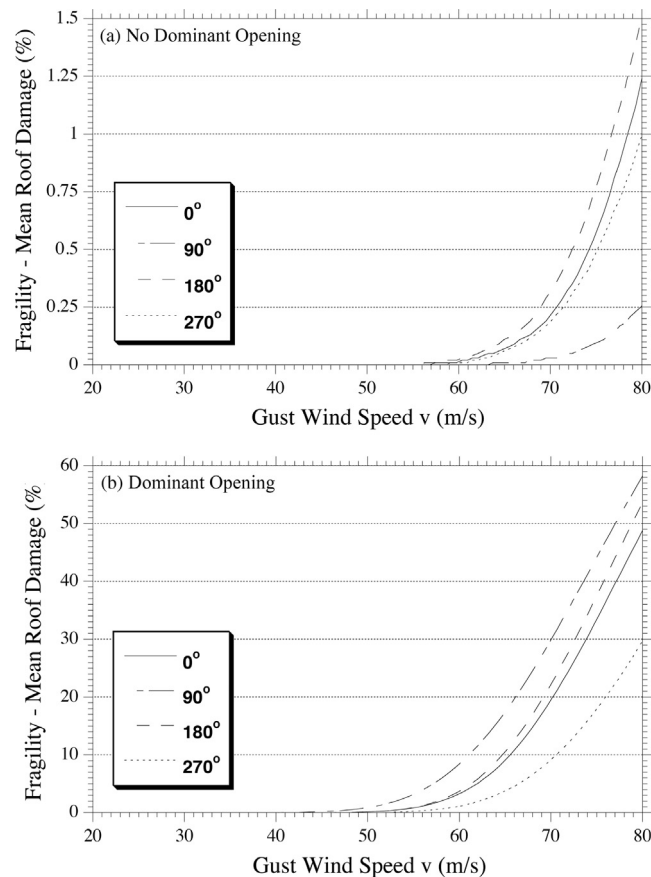

Fig. 11. Fragility curves with no construction defects, for four wind directions.

5.2. Simulation results

5.2.1. No construction defects

Fig. 11 shows fragility curves for the representative Brisbane/Melbourne house with and without dominant openings, for four orthogonal wind directions, and no defects. Fragility is measured in this case as mean extent of roof damage (loss of sheeting). Fig. 11 shows, for example, at a wind speed of 70 m/s a house with no dominant openings exhibits a damage of 0.25% at an orientation of 0°, while a house with a dominant opening shows damage of 20% for the same orientation, a factor of nearly two orders of magnitude larger." In nearly all cases fragility is more than an order of magnitude higher for the house with a dominant opening due to larger internal pressures as shown in Fig. 8. Fig. 11 shows that the wind from 0° and from 180° causes the highest impact to the building especially for higher wind speeds when effects from orthogonal directions are compared. The main reason for this is the higher external pressure over larger areas of the roof for these wind directions compared to the other wind direction as shown in Fig. 7.

It is observed from Table 5 that roof fastener failure is the dominant failure mode for all wind speeds. This is expected, as housing damage surveys reveal roof sheeting loss is mostly due to roof fastener failure (e.g., [32]).

5.2.2. Defects in construction

Construction defects are typically observed in most houses, so it is reasonable to assume that a more realistic fragility analysis will include construction defects as described in Section 4.3.4. The proportion of roof fastener, batten and sheeting loss are shown in Table 6 for houses with construction defects. When compared with Table 5, there are considerably more fastener and batten failures at lower wind speeds.

Table 7 shows the proportion of fastener and battens that fail in each roof zone (Fig. 12 shows the location of each zone), for a house

Table 5
Proportion of Failed Roof Fasteners, Battens and Sheets, No Defects and θ = 0°.

| Gust wind speed (v) m/s	Dominant opening			No dominant opening		
	Roof fasteners	Battens	Sheets	Roof fasteners	Battens	Sheets
30	0.00%	0.00%	0.00%	0.00%	0.00%	0.00%
40	0.00%	0.00%	0.00%	0.00%	0.00%	0.00%
50	0.09%	0.00%	0.10%	0.00%	0.00%	0.00%
60	1.49%	0.33%	2.00%	0.02%	0.00%	0.01%

Table 6
Proportion of failed roof fasteners, battens and sheets, with construction defects and $\theta = 0°$.

Gust wind speed (v) m/s	Dominant opening			No dominant opening		
	Roof fasteners	Battens	Sheets	Roof fasteners	Battens	Sheets
30	0.50%	0.05%	0.07%	0.24%	0.01%	0.01%
40	0.84%	0.23%	0.33%	0.43%	0.05%	0.06%
50	1.34%	0.68%	1.24%	0.65%	0.14%	0.17%
60	3.40%	2.05%	6.68%	0.91%	0.34%	0.42%

Table 7
Percentage of fasteners and battens failed in each roof zone for house with a dominant opening and construction defects, for a wind speed of 60 m/s.

Roof zone	$\theta = 0°$		$\theta = 90°$	
	Fasteners	Battens	Fasteners	Battens
1	4.9%	2.5%	1.9%	0.9%
2	1.4%	1.0%	2.4%	1.5%
3	1.7%	0.7%	2.2%	1.1%
4	2.9%	1.5%	2.0%	0.8%
5	2.4%	1.6%	1.4%	0.8%
6	2.8%	1.6%	1.5%	0.7%
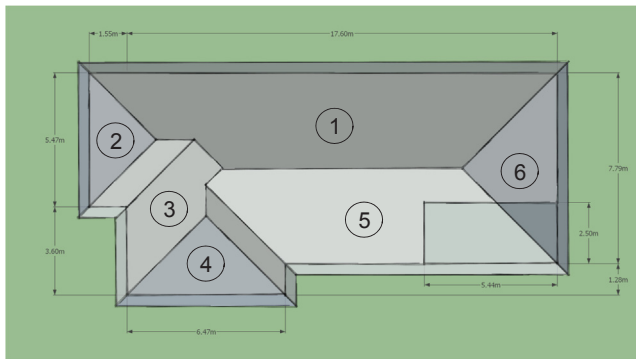
Fig. 12. Location of roof zones for use with Table 7.
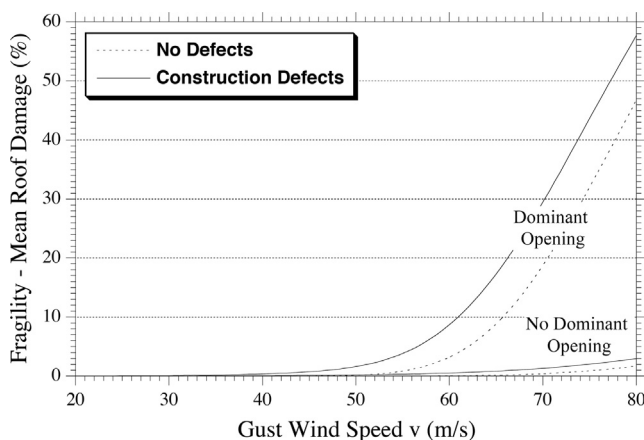
Fig. 13. Multi-directional fragility curves with and without construction defects.

with construction defects and a dominant opening at a wind speed of 60 m/s. Note that construction defects acts to distribute the failures more evenly across the entire roof, but Table 7 still shows that failures closely mirror that of the location of peak external suction pressures as shown in Fig. 7.

Fig. 13 shows the multi-directional wind fragility for the roof cladding and batten system for the representative house with and without construction defects. Construction defects increase fragility by up to 10% for high wind speeds, and reduce the damage threshold by 15 m/s. Clearly, the effect of construction defects is significant, and should be included in fragility modelling. A sensitivity analysis reveals that roof fastener and batten defects increases the fragility by approximately 45% and 85%, respectively. In this case, results are more sensitive to defects in batten-to-truss connections. However, if the defect rate of battens is halved to 1–3% (i.e., same as the defect rate for roof fasteners), the increase in fragility is similar to that observed for fastener defects.

For a building with construction defects, roof damage starts (assuming threshold damage is 0.5%) at wind speeds of 42 m/s and 59 m/s for a house with and without a dominant opening, respectively. In other words, the roof damage threshold wind speed is reduced by about 25% when the house experiences a dominant opening compared with a house without an opening. The main reason for this is the increase in internal pressure of a building with a dominant opening, which increases the wind load. According to Fig. 8, the mean internal pressure coefficients in a nominally sealed building changes from 0 for a building without a dominant opening to +0.65 for a building with a windward wall opening.

The fragility curve fitted to Fig. 13 uses a Weibull curve (e.g., [15,48]):

$$\Pr(DS\,|H) = \gamma \left\{ 1 - \exp\left[-\left(\frac{v}{e^\beta}\right)^{\frac{1}{\alpha}} \right] \right\} \quad v \leqslant 80\,\text{m/s}, \quad \Pr(DS\,|H) \leqslant 100\%$$

(8)

where γ, α and β are parameters that describe the shape and position of the vulnerability curve, see Table 8.

Wind roof damage data for houses in non-cyclonic regions are not available from open-source damage surveys or insurance data, which makes it difficult to validate models with real-world data. However, as expected the roof fragility for contemporary housing is lower than that of residential construction where all damage modes are considered (roof sheet failure, failed truss-to-wall connection, failed external walls, water ingress into failed doors and windows, debris impact, etc.). For example, the wind threshold for damage to contemporary residential construction in Brisbane considering all causes of damage is 15–20 m/s lower than that observed herein for roofing damage to Brisbane housing (e.g. [42,48]).

6. Loss modelling

Damage to the roof envelope results in the following losses:

- L_1: roof covering,
- L_2: roof framing,
- L_3: building interior,
- L_4: contents losses, and
- L_5: loss of use.

Other losses caused by clean-up, loss during reconstruction, extra demands on social services, etc. are not considered, although their

Table 8
Best-fit parameters for mean fragility functions.

Dominant opening during extreme winds	Construction defects	γ	α	β
No	No	2.49	0.072	4.376
No	Yes	4.38	0.148	4.398
Yes	No	54.03	0.086	4.325
Yes	Yes	80.67	0.118	4.349

effect on total losses may be significant for extreme wind events, their effect on average losses is not significant [48]. The average cost per new house (excluding land value) in southeast Australia is approximately $300,000 in 2016 Australian dollars [1].

Loss function are taken from models developed for residential construction in the United States by the Federal Emergency Management Agency [18]. It is assumed herein that Australian housing have similar loss characteristics to U.S. housing – housing in both countries are of timber construction, use similar materials for interiors, are of similar size, and contain similar electrical and mechanical systems. Moreover, the present analysis is less interested in a precise estimation of dollar losses, but is more concerned with the comparative effects that dominant openings and climate change have on damage risks.

6.1. Direct losses

6.1.1. Roof damage

Insurance data suggests that metal roof sheeting is entirely replaced if roof cover damage exceeds 5% [18]. Thus, the probability of loss associated with roof damage is

$$Pr(L_1 | DS = R_{damage}) = \begin{cases} R_{damage} & R_{damage} \leqslant 5\% \\ 1.0 & R_{damage} > 5\% \end{cases} \quad (9)$$

where R_{damage} is damaged roof area and L_1 is roofing replacement cost equal to 5.6% of housing cost for a single storey dwelling with a hip roof [18]. Note that this value, and subsequent costs estimates, includes a repair and remodelling cost adjustment factor of 1.25, and an overhead and profit factor of 1.20 to account for the additional costs associated with repair and remodelling due to "decrease in labor output typically associated with repair and remodelling work" [18]. If the threshold of full replacement of the roof is increased from $R_{damage} = 5\%$ to $R_{damage} = 50\%$, the economic risks calculated in the next Section reduce, in relative terms, by about 2%, hence, results are quite insensitive to the damage threshold for complete roof replacement.

6.1.2. Roof framing

The value of roof framing is $L_2 = 19.5\%$ of building replacement value, and the probability of economic loss associated with loss of roofing is [18]:

$$Pr(L_2 | DS = R_{damage}) = \begin{cases} R_{damage} & R_{damage} \leqslant 25\% \\ 1.0 & R_{damage} > 25\% \end{cases} \quad (10)$$

6.1.3. Interior losses

Interior losses include direct costs of ceiling, wall, floor and other non-structural components. The probability of interior economic loss associated with loss of metal roof sheeting is [18]:

$$Pr(L_3 | DS = R_{damage}) = \begin{cases} 0.0 & R_{damage} < 0.5\% \\ 0.1 & R_{damage} = 0.5\% \\ 0.036 R_{damage} + 0.1 & 0.5\% < R_{damage} \leqslant 25\% \\ 1.0 & R_{damage} > 25\% \end{cases} \quad (11)$$

It is assumed that interior loss is 10% following failure of the first piece of roof sheeting ($R_{damage} = 0.5\%$), with interior losses then increasing linearly up to 100% at 25% failed or missing roof cover. According to HAZUS [18], 48% of house building value is assigned to internal construction, 4.5% to electrical systems, 13.5% to mechanical systems (heating, cooling), and 6% to kitchen cabinets and shelving. Total interior replacement cost is $L_3 = 72\%$ of building replacement value.

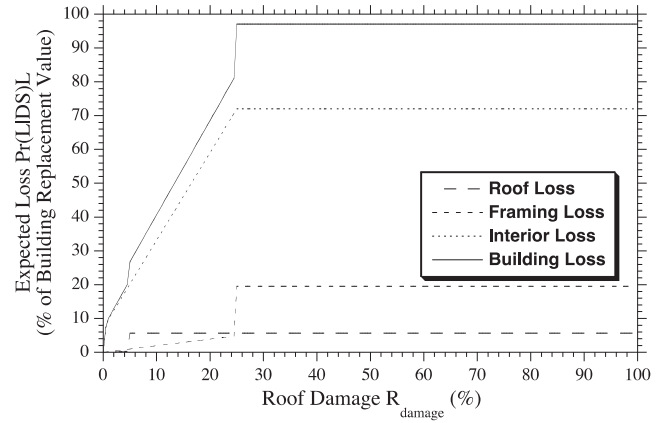Total expected building loss conditional on damage level is

Fig. 14. Components of building loss.

$$Pr(L_{building} | DS = R_{damage}) L_{building} = \sum_{i=1}^{3} Pr(L_i | DS = R_{damage}) L_i \quad (12)$$

Fig. 14 shows that losses accumulate rapidly for low levels of roof damage.

6.1.4. Contents losses

HAZUS [18] recommends that contents losses are similar to interior losses because water ingress from a small loss of roofing may lead to significant damage to contents. This leads to:

$$Pr(L_4 | DS = R_{damage}) = \begin{cases} 0.04 R_{damage} & R_{damage} \leqslant 25\% \\ 1.0 & R_{damage} > 25\% \end{cases} \quad (13)$$

HAZUS [18] assumes that $L_4 = 50\%$ of building replacement value.

6.2. Loss of use

The annual likelihood of loss of use arising from a damaged building is [18]:

$$Pr(L_5 | DS) = \frac{N_{lou}(Pr(L_{building} | DS) L_{building}) \cdot Mod(Pr(L_{building} | DS) L_{building})}{365} \quad (14)$$

where $N_{lou}()$ is building loss of use (days) taking into account delays in decision-making, financing, inspection, etc., and $Mod()$ is a loss of use multiplier modelled as a function of expected building loss $Pr(L_{building} | DS) L_{building}$ given by Eq. (12). According to HAZUS [18], $N_{lou} = 0, 5, 120, 360$ and 720 days and $Mod() = 0.0, 0.0, 0.5, 1.0$ and 1.0, for expected building loss of 0%, 2%, 10%, 50% and 100%, respectively. The loss of use multipliers "take into account the fact that homeowners can remain in their homes when buildings have slight to moderate damage" [18]. If we assume that a weekly rent for a house is $400 per week [2], then annual loss of use is approximately $L_5 = \$21,000$.

7. Climate change impact risks

The annual risk for a climate scenario at time t is

$$E_{annual}(t) = \int_0^\infty \left[\frac{dF_v(v, t)}{dv} \right] \frac{0.125 \sum_{j=1}^{8} \lfloor Pr(DS | H = M_{dj}v) \sum_{i=1}^{5} Pr(L_i | DS) L_i \rfloor}{(1 + r)^t} dv \quad (15)$$

where $F_v(v,t)$ is the time-dependent cumulative function for annual maximum wind speed given by Eq. (4), M_d is the wind speed directionality multiplier for the eight cardinal directions given in Table 9 [3], $Pr(DS|H = v)$ is wind fragility given by Eq. (8), $Pr(L_i|DS)$ is loss

Table 9
Wind speed direction multiplier [3].

Cardinal direction	Brisbane	Melbourne
N	1.0	1.0
NE	1.0	0.85
E	1.0	0.80
SE	1.0	0.80
S	1.0	0.85
SW	1.0	0.90
W	1.0	1.0
NW	1.0	0.95

likelihood given by Eqs. (9)–(14), L_i is the maximum loss for loss i, and r is the discount rate. Eq. (15) assumes that damage is caused by the largest wind event in any calendar year, which will slightly under-estimate damage risks in the event of a (very unlikely) lesser damaging event occurring in the same season. For Brisbane, peak wind speed is equally likely from any direction (see Table 9). However, for Melbourne Table 9 shows that the wind directionality multiplier varies for the eight cardinal directions. In this case, wind direction is assumed uniformly distributed in 10° increments between 0° and 360° to allow for variability of wind speed with wind direction.

The cumulative expected loss (or risks) over the 50-year life of the building (2016–2066) is:

$$E(L) = \sum_{t=2016}^{2066} E_{annual}(t) \tag{16}$$

where $E_{annual}(t)$ is the present value given by Eq. (15). The selection of the discount rate for climate impact assessments is not clear; for example, see Dasgupta [10] and Stewart [52]. All economic risks are presented as 2016 Australian dollars and discount rate is r = 4%.

Wind speeds in excess of 60 m/s have an average recurrence interval of nearly 50,000 years in non-cyclonic regions of Australia (AS1170.2 2011). Hence, wind fragilities for wind speeds above 60 m/s have little effect on economic risks.

Table 10 shows the existing level of annual economic risk per house as percentage of house replacement value for losses L_1 to L_4 (E_{damage}) and annual loss of use (days) risk using L_5 (E_{use}) in Eq. (15), for no change in wind field. Annual economic risks are 0.00–0.05% for Brisbane and 0.00% for Melbourne, for houses without construction defects. In the more realistic case where construction defects are considered, annual economic risks increase to 0.01–0.30% for Brisbane and 0.00–0.01% for Melbourne. Economic risks are lower for Melbourne due to lower gust hazard when compared to Brisbane. Not surprisingly, if a dominant opening occurs on the windward wall, economic risks increase by up to twenty-fold. A typical house with construction defects increases economic risk more than sixfold when compared to the defect-free house.

The cumulative economic risks over the 50-year design life of the building calculated from Eq. (16) are shown in Table 11 for a 4% discount rate, a house with typical construction defects, and using the 10th, median and 90th percentile changes in wind speed given in

Table 10
Annual risks for no change in wind field.

Dominant opening during extreme winds	Construction defects	Brisbane		Melbourne	
		$E_{annual\text{-}damage}$	$E_{annual\text{-}use}$	$E_{annual\text{-}damage}$	$E_{annual\text{-}use}$
No	No	0.00%	0.00 days	0.00%	0.00 days
No	Yes	0.01%	0.01 days	0.00%	0.00 days
Yes	No	0.05%	0.12 days	0.00%	0.00 days
Yes	Yes	0.30%	0.73 days	0.01%	0.00 days

Table 11
Cumulative 50-year economic risks, for construction defects and discount rate of 4%.

	No dominant opening			Dominant opening		
	10th	Median	90th	10th	Median	90th
Brisbane						
No change	–	$980	–	–	$20,780	–
RCP2.6	$910	$980	$1060	$18,810	$20,780	$22,960
RCP4.5	$760	$930	$1010	$18,080	$19,590	$21,660
RCP8.5	$830	$910	$1040	$17,000	$19,180	$22,520
Melbourne						
No change	–	$140	–	–	$760	–
RCP2.6	NA	NA	NA	NA	NA	NA
RCP4.5	NA	NA	NA	NA	NA	NA
RCP8.5	$125	$135	$160	$660	$730	$900

Table 1. A house that experiences a dominant opening will experience damage losses of about $1000 and $22,500 by 2066 for Melbourne and Brisbane, respectively. These are relatively large losses for Brisbane. A properly designed house with typical construction defects and no dominant openings should suffer negligible losses due to roof cladding damage. A changing climate will slightly reduce median losses for Brisbane. However, there is a 10% chance (90th percentile) that climate change-induced wind speeds will increase, hence, losses may increase by up to 6–8% and 14–18% for Brisbane and Melbourne, respectively. Generally, however, a changing climate is more likely to reduce wind cladding damage losses for Brisbane and Melbourne as wind speeds are more likely to be reduced (see Table 1).

As discussed in Section 5.2.2, fragilities are sensitive to construction defects. Hence, a sensitivity analysis is conducted to assess the effect of defect rates on the existing level of annual economic risk for houses in Brisbane assuming that a dominant opening occurs on the windward wall. If the defect rate of battens is halved to 1–3% (i.e., same as the defect rate for roof fasteners), the annual economic risk for Brisbane reduces, in relative terms, by 47%. If defect rates for roof fasteners and battens are then halved to 0.5–1.5%, the annual economic risk for Brisbane shown in Table 10 reduces to 0.075% – i.e., is 50% higher than defect free construction. As noted in Section 4.3.4, this highlights the importance of defect rates on housing damage –more research is needed to better characterise the rate and consequences of defective construction.

Future work will incorporate the fragility of roofing described herein with a stochastic and spatially varying analysis of roof truss-to-wall connection. Truss-to-wall connections in non-cyclonic regions in Australia have been found to suffer from inadequate design and construction, leading to higher probability of failure and significant loss of roof covering. Added to this will be losses resulting from water ingress into failed windows and doors. This will lead to higher, and more realistic, economic losses resulting from extreme wind events.

8. Conclusions

A risk analysis was conducted to assess the economic impact of roof cladding damage for a typical contemporary (new) Australian house in a non-cyclonic region subject to extreme wind loading. The economic risks were calculated as the product of hazard likelihood, fragility, and loss over the 50-year design life of a house. The dominant failure modes considered in this case study are (i) roof cladding failure, and (ii) batten-to-truss connection failure. The effect of defective construction at connections is also considered. Monte-Carlo simulation and structural reliability methods were used to stochastically model spatially varying pressure coefficients, roof component failure, load re-distribution and spatial variability of damage across the roof. This enabled fragility curves to be developed that quantify the extent of roof cover damage with wind speed. The risk analysis found that a properly

designed house with typical construction defects and no dominant openings should suffer negligible losses due to roof cladding damage. However, these losses increase up to twenty-fold if a dominant opening occurs in the building envelope. There is a 10% chance that a changing climate will increase expected losses for Brisbane and Melbourne by 6–18% over the next 50 years. Finally, to better inform fragility analyses there is a clear need for the collection of field data on construction defects.

Acknowledgements

Appendix A. Supplementary material

Supplementary data associated with this article can be found, in the online version, at http://dx.doi.org/10.1016/j.engstruct.2018.05.125.

References

[1] Australian Bureau of Statistics. A twenty year history of the cost of building a new house. Belconnen, Australia; 2008.
[2] Australian Bureau of Statistics. Housing Occupancy and Costs, 2013-14. Australian Bureau of Statistics, 16 October, 2015, Belconnen, Australia; 2015.
[3] AS/NZS1170.2. Structural design actions. Part 2: Wind actions, standards Australia, Sydney; 2011.
[4] AS4055-2012. Wind loads for houses. Standards Australia, Sydney.
[5] BITRE. About Australia's regions. Bureau of infrastructure, transport and regional economics, Canberra; 2008.
[6] Bjarnadottir S, Li Y, Stewart MG. Regional loss estimation due to hurricane wind and hurricane-induced surge considering climate variability. Struct Infrastruct Eng 2014;10(11):1369–84.
[7] Boughton G, Henderson D, Ginger J, Holmes J, Walker G, Leitch C, et al. Tropical Cyclone Yasi: structural damage to buildings. Cyclone Testing Station. James Cook University. Report TR57; 2011.
[8] Boughton GN, Falck DK, Vinh Nghi Duong A, Pham S, Nguyen A. Static testing of batten connections at University of Western Australia. Cyclone Testing Station. James Cook University. Report TR62; 2015.
[9] Cui W, Caracoglia L. Exploring hurricane wind speed along US Atlantic coast in warming climate and effects on predictions of structural damage and intervention costs. Eng Struct 2016;122:209–25.
[10] Dasgupta P. Discounting climate change. J Risk Uncertain 2008;37(2–3):141–69.
[11] Dowdy A et al. East coast cluster report, climate change in australia projections for australia's natural resource management regions: cluster reports. In: Ekström M et al., editors. CSIRO and Bureau of Meteorology, Australia; 2015.
[12] Gavanski E, Kopp GA, Hong HP. Reliability analysis of roof sheathing panels on wood-frame houses under wind loads in Canadian cities. Can J Civ Eng 2014;41:717–27.
[13] Ginger JD, Letchford CW. Characteristics of large pressures in regions of flow separation. J Wind Eng Ind Aerodyn 1993;49:301–10.
[14] Ginger JD, Holmes JD, Kim PY. Variation of internal pressure with varying sizes of dominant openings and volumes. J Struct Eng 2010;136(10):1319–26.
[15] Ginger J, Henderson D, Edwards M, Holmes J. Housing damage in windstorms and mitigation for Australia. In: Proceedings of 2010 APEC-WW and IG-WRDRR Joint Workshop: Wind-Related Disaster Risk Reduction Activities in Asia-Pacific Region and Cooperative Actions; 2010. p. 1–18.
[16] Ginger J, Henderson D, Humphreys M, Konthesingha C, Stewart MG. Wind loads on the frames of industrial buildings. Aust J Struct Eng 2015;16(2):169–78.
[17] Grose M et al. Southern slopes cluster report. Climate Change in Australia Projections for Australia's Natural Resource Management Regions: Cluster Reports. In: Ekström, M et al., editors. CSIRO and Bureau of Meteorology, Australia; 2015.
[18] HAZUS. Multi-hazard loss estimation methodology – hurricane model, Hazus–MH 2.1 Technical manual. Federal emergency management agency. Mitigation Division. Washington, D.C.; 2014.
[19] Henderson D, Ginger J. Vulnerability of JCU Group 4 House to cyclonic wind loading, CTS Report TS614 for Geoscience Australia. Australia: James Cook University; 2005.
[20] Henderson DJ, Ginger JD. Vulnerability model of an Australian high-set house subjected to cyclonic loading. Wind Struct 2007;10(3):269–85.
[21] Henderson DJ, Ginger JD. Role of building codes and construction standards in windstorm disaster mitigation. Australian J Emergency Manage 2008;23(2):40–46.
[22] Henderson DJ, Ginger JD. Response of pierced fixed corrugated steel roofing systems subjected to wind loads. Eng Struct 2011;33:3290–8.
[23] Henderson D, Williams C, Gavanski E, Kopp GA. Failure mechanisms of roof sheathing under fluctuating wind loads. J Wind Eng Ind Aerodyn 2013;114:27–37.
[24] Holmes JD. Wind loads and limit states design. Civil Eng Trans Inst Eng Australia 1985;CE27(1):21–6.
[25] Holmes JD. Wind loading of structures. London, UK: Spon Press; 2007.
[26] Hong HP, He WX. Effect of human error on the reliability of roof panel under uplift wind pressure. Struct Saf 2015;52:54–65.
[27] Kirwin B. A guide to practical human reliability assessment. London: Taylor & Francis; 1994.
[28] Konthesingha C, Stewart MG, Ryan PC, Ginger JD, Henderson DJ. Reliability based vulnerability modelling of metal-clad industrial buildings to extreme wind loading for cyclonic regions. J Wind Eng Ind Aerodyn 2015;147:176–85.
[29] Lee KH, Rosowsky DV. Fragility assessment for roof sheathing failure in high wind regions. Eng Struct 2005;27(857):868.
[30] Leicester RH. Engineered performance for timber construction. NZ Timber Des J 1995;4(9):2–4.
[31] Leicester RH, Reardon G. Impact Stat Tracy Opportunity Missed Aust Meteorol Oceanogr J 2010;60:207–12.
[32] Leitch C, Ginger J, Harper B, Kim P, Jayasinghe N, Somerville L. Investigation of performance of housing in brisbane following storms on 16 and 19 November 2008. Technical Report No. 55. Cyclone Testing Station. James Cook University; 2009.
[33] Li Y, Ellingwood BR. Hurricane damage to residential construction in the US: importance of uncertainty modeling in risk assessment. Eng Struct 2006;28(7):1009–18.
[34] Li Y, Stewart MG. Cyclone damage risks caused by enhanced greenhouse conditions and economic viability of strengthened residential construction. Nat Hazard Rev 2011;12(1):9–18.
[35] Lysaght. TOPSPAN Design and Installation Guide for Building Professionals. Bluescope Lysaght, Australia; 2014.
[36] Mahendran M. Fatigue behaviour of corrugated roofing under cyclic wind loading. Civil Eng Trans, IEAust 1990;32(4):219–26.
[37] Mahendran M, Tang RB. Pull-out strength of steel roof and wall cladding systems. J Struct Eng 1998;124(10):1192–201.
[38] Nishijima K, Maruyama T, Graf M. A preliminary impact assessment of typhoon wind risk of residential buildings in japan under future climate change. Hydrol Res Lett 2012;6(1):23–8.
[39] Parackal KI, Humphreys MT, Ginger JD, Henderson DJ. Wind loads on contemporary Australian housing. Aust J Struct Eng 2016;17(2):136–50.
[40] Parackal K, Mason M, Henderson D, Stark G, Ginger J, Somerville L et al. Investigation of Damage: Brisbane, 27 November 2014 Severe Storm Event, Technical Report No. 60, Cyclone Testing Station, James Cook University, February 2015; 2015.
[41] Sadek F, Simiu E. Peak non-Gaussian wind effects for database-assisted low rise building design. J Eng Mech 2002;128:530–9.
[42] Schofield A, Arthur C, Cechet B. Assessing the impacts of tropical cyclone tracy on residential building stock – 1974 and 2008. Aust Meteorol Oceanogr J 2010;80:213–9.
[43] Seo D-W, Caracoglia L. Exploring the impact of "climate change" on lifetime replacement costs for long-span bridges prone to torsional flutter. J Wind Eng Ind Aerodyn 2015;140(May):1–9.
[44] Stewart MG. Structural reliability and error control in reinforced concrete design and construction. Struct Saf 1993;12:277–92.
[45] Stewart MG. Modelling human performance in reinforced concrete beam construction. J Constr Eng Manage ASCE 1993;119(1):6–22.
[46] Stewart MG, Melchers RE. Probabilistic risk assessment of engineering systems. London: Chapman & Hall; 1997.
[47] Stewart MG, Wang X. Risk assessment of climate adaptation strategies for extreme wind events in Queensland. CSIRO Climate Adaptation Flagship, Canberra; 2011.
[48] Stewart MG, Wang X, Willgoose GR. Direct and indirect cost and benefit assessment of climate adaptation strategies for housing for extreme wind events in Queensland. Nat Hazard Rev 15(4):04014008(12).
[49] Stewart MG. Risk and economic viability of housing climate adaptation strategies for wind hazards in southeast Australia. Mitig Adapt Strat Glob Change 2014;20(4):601–22.
[50] Stewart MG, Deng X. Climate impact risks and climate adaptation engineering for built infrastructure. ASCE-ASME J Risk Uncertainty in Eng Syst Part A: Civil Eng 2015;1(1):04014001.
[51] Stewart MG, Ryan PC, Henderson DJ, Ginger JD. Fragility analysis of roof damage to industrial buildings subject to extreme wind loading in non-cyclonic regions. Eng Struct 2016;128:333–43.
[52] Stewart MG. Climate change impact assessment of metal-clad buildings subject to extreme wind loading in non-cyclonic regions. Sustain Resilient Infrastruct 2016;1(1–2):32–45.
[53] van de Lindt JW, Dao TN. Performance-based wind engineering for wood-frame buildings. J Struct Eng 2009;135(2):169–77.
[54] van de Lindt JW, Nguyen Dao T. Construction quality issues in performance-based wind engineering: effect of missing fasteners. Wind Struct 2010;13(3):221–34.
[55] Vickery PJ, Skerlj PF, Lin J, Twisdale LA, Young MA, Lavelle FM. HAZUS-MH hurricane model methodology. II: Damage and loss estimation. Nat Hazard Rev 2006;7(2):94–103.
[56] Vickery PJ, Banik S. Modelling the progressive failure of buildings in high winds, transactions SMiRT 23. In: 23rd Conference on structural mechanics in reactor technology, Manchester, United Kingdom, Paper ID 810; 2015.
[57] Wang C-H, Wang X, Khoo YB. Extreme wind gust hazard in Australia and its sensitivity to climate change. Nat Hazards 2013;67(2):549–67.
[58] Webb LB, Hennessy K. Climate change in Australia: projections for selected Australian cities. CSIRO and Bureau of Meteorology, Australia; 2015.
[59] Zhang S, Nishijima K, Maruyama T. Reliability-based modelling of typhoon induced wind vulnerability for residential buildings in Japan. J Wind Eng Ind Aerodyn 2014;124:68–81.